Smart Divert: A New Entry, Descent, and Landing Architecture

AE8900 MS Special Problems Report
Space Systems Design Lab (SSDL)
Guggenheim School of Aerospace Engineering
Georgia Institute of Technology
Atlanta, GA

Author:
Michael J. Grant

Advisor:
Dr. Robert D. Braun

May 2, 2008

Smart Divert: A New Entry, Descent, and Landing Architecture

Michael J. Grant[1] and Robert D. Braun[2]
Georgia Institute of Technology, Atlanta, GA, Zip, 30332

Mars robotic landing site selection has been a compromise between scientific interest and safety. Due to the rather large landed footprint major axis lengths of Viking, Pathfinder, Mars Exploration Rovers, and Phoenix, mission designers have been forced to orient the landed ellipse in vast, relatively flat areas to provide high probability of landing success. Scientists are interested in exploring more geologically interesting areas that contain many hazards, including sloping terrain, craters, and rocks. Smart Divert provides a new entry, descent, and landing architecture that could allow robotic missions to safely land in hazardous terrain. Smart Divert consists of a ballistic entry followed by supersonic parachute deployment. After parachute release, the vehicle diverts to one of many predefined, fuel-optimal safe zones. Smart Divert performance and entry design is discussed and is followed by a discussion of Smart Divert for random terrain. An initial assessment of optimal landing site arrangement is performed and an example of the usefulness of Smart Divert is performed for real terrain using Phoenix landing site rock count data.

Nomenclature

$\underline{a}$	=	Acceleration vector
$\underline{g}$	=	Local gravity vector
J	=	Cost function
t_0	=	Time of divert initiation
t_f	=	Final touchdown time
t_{go}	=	Time-to-go
Γ	=	Weighting on time-to-go
$\underline{\Delta r}$	=	Position of vehicle relative to target
$\underline{\Delta v}$	=	Velocity of vehicle relative to target
AGL	=	Above ground level
DOF	=	Degree-of-freedom
DDOR	=	Delta Differential One-Way Ranging
DGB	=	Disk-gap-band
EDL	=	Entry, descent, and landing
HiRISE	=	High Resolution Imaging Science Experiment
JPL	=	Jet Propulsion Laboratory

[1] Graduate Research Assistant, Guggenheim School of Aerospace Engineering, AIAA Student Member.
[2] David and Andrew Lewis Associate Professor of Space Technology, Guggenheim School of Aerospace Engineering, AIAA Fellow.

MER = Mars Exploration Rovers
MRO = Mars Reconnaissance Orbiter
MSL = Mars Science Laboratory
PMF = Propellant mass fraction
RCS = Reaction control system
TCM = Trajectory correction maneuver

I. Introduction

TO date, entry, descent, and landing (EDL) mission designers have been forced to trade safety and scientific interest when choosing the landing site of various Mars landers. Past missions have resulted in rather large landed footprint major axis lengths ranging from 200 km (Viking, Pathfinder) to 80 km (Mars Exploration Rovers).[1] Generally, scientifically interesting landing sites are not flat and contain many hazards including significant variation in terrain elevation, craters, and rocks. Hence, it is the interest of scientists to visit these dangerous regions on Mars. However, mission designers must ensure that the majority of the landed ellipse encapsulates safe terrain. This leads the mission designers to orient the landing site ellipse over vast flat regions of Mars. It would be very beneficial if science could dominate the choice of landing site location. This could be achieved with greater landed accuracy. In order to achieve improved accuracy, hypersonic guidance will be used for the first time at Mars on the Mars Science Laboratory (MSL). The modified Apollo guidance utilizes only the terminal phase of the Apollo entry guidance and provides a landed footprint 20 km long in major axis through modulation of the lift vector.[2] This allows MSL to travel to more dangerous and scientifically interesting sites. However, the implementation of hypersonic guidance greatly increases complexity and cost of the mission as compared to previous ballistic, unguided missions. Also, mission designers are still required to ensure the majority of the 20 km landed ellipse is over safe terrain. Smart Divert may provide a simple, low cost entry, descent, and landing architecture for landing in dangerous terrain. Smart Divert consists of a ballistic entry followed by supersonic disk-gap-bank (DGB) parachute deployment at Mach 2.2, consistent with previous missions. At Mach 0.8, the parachute is released and the vehicle propulsively diverts to a fuel-optimal safe zone identified prior to EDL.

II. Planar Example

The visualization of 3D divert trajectories is quite difficult. In order to conceptually understand Smart Divert, a simple planar example was constructed. The entry flight path angle was varied to produce a ballistic parachute deploy line (all trajectories are confined to a plane) as shown in a and b of Figure 1. Note that the downrange spread at parachute deploy is only approximately 10 km. This is unrealistically small and is only used to conceptually demonstrate Smart Divert. In Figure 1a, a single site is located at 0 km downrange. After the ballistic entry and parachute phase, each trajectory diverts to the target site on a fuel optimal trajectory. The diverts that initiate far uprange must divert a long distance, requiring more fuel than the diverts that initiate closer to the target. In order to reduce the propellant mass fraction (PMF) required by the uprange trajectories, a second site was added uprange and may be seen in Figure 1b. As can be seen, the vehicle evaluates which site is fuel optimal and flies to

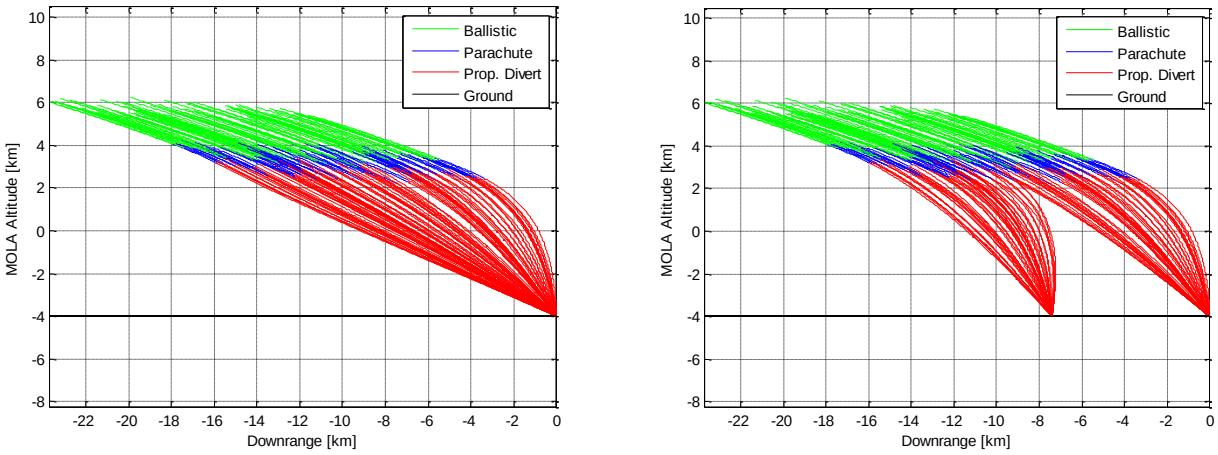

a) **b)**

Figure 1: Example Divert to One and Two Sites

that site. Hence, the uprange trajectories identified the uprange site as fuel optimal and diverted to that site.

III. Simulation Development

In order to have a flexible conceptual design tool that is capable of rapidly trading various EDL scenarios, a 3 degree-of-freedom (DOF) Mars entry simulation was developed in Matlab. The Matlab code was autocoded into a C-Mex file using the Matlab Real-Time Workshop, which dramatically reduces the execution time by an approximate factor of 35. The equations of motion were expressed in an inertial, Cartesian space. This method avoids singularities associated with angular derivatives (*e.g.*, rate of change in latitude, longitude, flight path angle, etc) as the vehicle's velocity approaches zero (*e.g.*, during terminal descent). A spherical, rotating planet with a spherical mass distribution was also assumed.

In order to assess the performance of Smart Divert, a Monte Carlo environment was developed with dispersions similar to those simulated for MSL.[3] Atmospheric properties, vehicle properties, parachute aerodynamic drag coefficient, and delivery accuracy to Mars are dispersed and are shown in Table 1 and Table 2. An MSL-class DGB parachute with a diameter of 19.5 m and drag coefficient profile shown in Figure 2 was used. Note the drag bucket near Mach 1 is captured and reduces parachute performance. This will be an important consideration for low parachute deployment altitudes performed in subsequent analyses. The delivery accuracy was quantified as an entry state covariance at ten minutes prior to entry interface provided by the Jet Propulsion Laboratory (JPL) for MSL assuming the trajectory correction maneuver (TCM) 5 was performed. This covariance corresponds to state-of-the-art interplanetary navigation capability in which the vehicle is spin stabilized, delta differential one-way ranging (DDOR) is used, and a delivery error reducing TCM 5 is performed. The corresponding MSL 3σ entry flight path angle uncertainty is approximately 0.1^o as opposed to the Phoenix 3σ entry flight path angle uncertainty of 0.21^o.

A set of dispersed atmospheres was generated using MarsGRAM 2005. The parameters used to generate the atmospheres are shown in Table 2. The resulting atmosphere density profiles, normalized by the nominal density profile with a

Table 1: MarsGRAM 2005 Parameters

Parameter	Value / Range
Latitude [deg]	-40.60
Longitude [deg]	-62.90
Date	26 Jul 2010
Dusttau	0.1-0.9

Table 2: Monte Carlo Dispersions

Parameter	Nominal	Distribution	3σ or min/max
Entry State	MSL Nominal	Entry Covariance	Entry Covariance
C_a Multiplier	1	Gaussian	3%
Entry Mass [kg]	2196.0	Gaussian	2.0
Atmosphere Dispersion Seed	0	Uniform	1/29999
Atmosphere Update Distance [km]	0.5	Uniform	0.5/5.0
Dusttau	0.45	Uniform	0.1/0.9
Supersonic Parachute Drag	C_D Profile	Uniform	-10%/+10%
Terminal Descent Engine I_{sp} [sec]	194	Uniform	-0.67%/+0.67%

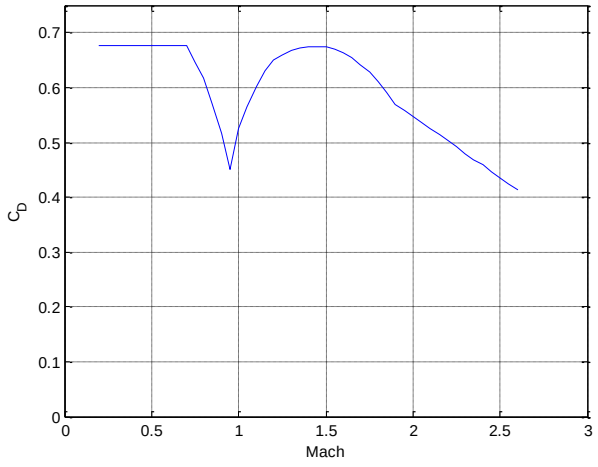

Figure 2: Drag Coefficient vs. Mach for DGB Parachute

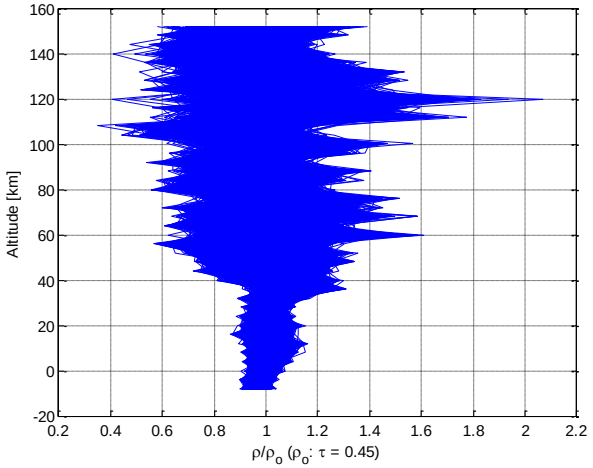

Figure 3: Atmosphere Density Profiles

Dusttau of 0.45, may be seen in Figure 3. As expected, large variations occur in the upper atmosphere. Perfect navigation throughout the EDL phase was also assumed.

IV. Divert Guidance

At Mach 0.8, the parachute is released and the propulsive terminal descent phase is initiated in which the vehicle diverts from its current location to the fuel optimal safe zone. The identification of the fuel optimal safe zone could be accomplished in two ways. First, a guidance algorithm could be used along with simplified equations of motion propagated onboard the vehicle. The fuel optimal safe zone could then be chosen autonomously after evaluating the propellant required to divert to each possible safe zone. This method was employed for this analysis. Alternatively, the selection of the divert site could be pre-selected by the ground. Due to the simplicity of ballistic entries, the distance traveled downrange could possibly be inferred by the entry acceleration profile. For example, the peak deceleration loads could potentially be used to identify where along the major axis the vehicle is likely located. From this estimated location, the vehicle could then divert to the corresponding fuel optimal safe zone identified by previous analysis on the ground, eliminating the need for complicated, real-time, onboard analysis.

A closed-form, analytic, fuel optimal control algorithm (D'Souza guidance) has been identified as a fuel optimal terminal descent control law for conceptual design.[4,5] The algorithm assumes a planar, non-rotating planet with negligible atmospheric forces compared to gravity and thrust. The altitude is also assumed to be much smaller than the radius of the planetary body. These assumptions are quite reasonable during terminal descent where the vehicle is close to the ground and traveling at subsonic speeds. The analytic D'Souza guidance provides a fuel-optimal, propulsive control law to perform the divert maneuver from the current time, t_0, to the final touchdown time, t_f, by minimizing the performance index shown in Eq. (1) where the weighting on time-to-go, Γ, is set initially to zero. The analytic control law is shown to be given by Eq (2), where the time to go, t_{go}, is the real positive root of Eq (3). $\underline{\Delta r}$ and $\underline{\Delta v}$ correspond to the relative position and velocity of the vehicle with respect to the target, respectively, as defined by D'Souza.[5] $\underline{a}$ corresponds to the vehicle acceleration vector, and $\underline{g}$ corresponds to the local gravity vector. The required thrust vector may then be easily obtained from the vehicle's current mass.

$$J = \Gamma t_f + \frac{1}{2}\int_{t_0}^{t_f} \left(\underline{a}^T \underline{a}\right) d\tau \tag{1}$$

$$\underline{a} = \frac{-4\underline{\Delta v}}{t_{go}} - \frac{6\underline{\Delta r}}{t_{go}^2} - \underline{g} \tag{2}$$

$$\left(\Gamma - \frac{g^2}{2}\right) t_{go}^4 - \left(2\underline{\Delta v}^T \underline{\Delta v}\right) t_{go}^2 - \left(12\underline{\Delta v}^T \underline{\Delta r}\right) t_{go} - 18\underline{\Delta r}^T \underline{\Delta r} = 0 \tag{3}$$

Immediately prior to initiating the divert, the vehicle evaluates the fuel optimality of each safe zone by propagating simplified equations of motion using the D'Souza guidance. Certain fuel optimal trajectories go through the surface of the planet. If this occurs during the evaluation of a trajectory to a specified safe zone, Γ is increased until a feasible trajectory that remains above the surface is found. An increase in Γ results in an increase weighting on the final time, resulting in more direct trajectories that remain above the surface at the penalty of increased fuel consumption.

The analytic nature of the control law is computationally inexpensive (relative to other guidance algorithms) and allows for rapid execution of Monte Carlos. A maximum thrust to weight ratio of 3 was used for the propulsive terminal descent (consistent with historical Mars robotic monopropellant hydrazine terminal descent systems).[6] Consequently, the thrust was limited if the analytic D'Souza algorithm commanded more thrust than permitted by the thrust to weight constraint. Navigation is assumed to be perfect throughout EDL. Using the D'Souza guidance algorithm and perfect EDL navigation, the miss distance of the vehicle at touchdown to the target is approximately 5 m. Hence, the landed accuracy of the vehicle is governed by navigation error. It has been shown that in order to achieve pinpoint landing accuracy (sub-100 m), terrain-relative navigation and a reduction in map-tie error will be required.[4] For Smart Divert, the landed accuracy dictates how large the safe zones must be to ensure a safe landing.

V. Conceptual Understanding of Smart Divert Performance

For dispersed trajectories, the flight path angle, altitude, and divert distance will vary. However, it is important to gain an understanding of the reasonable bounds of Smart Divert. For any given dispersed trajectory, the fuel-optimal divert site may be located along or against the natural direction of motion of the vehicle. As an average for this analysis, the vehicle is assumed to be traveling vertically downward at Mach 0.8 (immediately after parachute jettison). The altitude above the ground in which the divert is initiated was varied from 4-12 km and the horizontal distance of the divert was varied from 0-50 km. The resulting PMF for the various combinations of divert initiation altitudes and horizontal divert distances may be seen in Figure 4. The white region corresponding to the altitude of divert initiation between 4-12 km indicates divert trajectories that require a thrust-to-weight ratio larger than 3 or maximum Mach values larger than 0.8. Such cases are considered infeasible when performing a propulsive divert in a landing configuration. As expected, an increase in horizontal divert distance requires a higher divert initiation altitude. This ratio provides an effective glide slope of 3:1 for the divert. It is also important to note that initiating the divert at a higher altitude slightly increases the required PMF for the same horizontal divert distance. Thus, the vehicle should initiate the divert at as low of an altitude as possible.

In order to feasibly implement Smart Divert as a new EDL architecture, the propellant required to perform the required diverts must be maintained at a reasonable level. Previous EDL missions that require only a safe landing on the surface of Mars typically employ a variation of a gravity turn. The PMF required to perform a gravity turn is approximately 0.15. This is consistent with the 4 km altitude divert of 0 km. In order to feasibly implement Smart Divert, the propellant required should stay small and not double the required propellant to perform a gravity turn. Therefore, the vehicle should not divert more than 10 km to ensure the PMF required to perform the divert is less than 0.3. Since the vehicle should start the divert as low as possible, the vehicle should start the divert around 5 km above ground level (AGL) to divert a maximum of 10 km. This would allow sufficient timeline to perform the divert and other final EDL events.

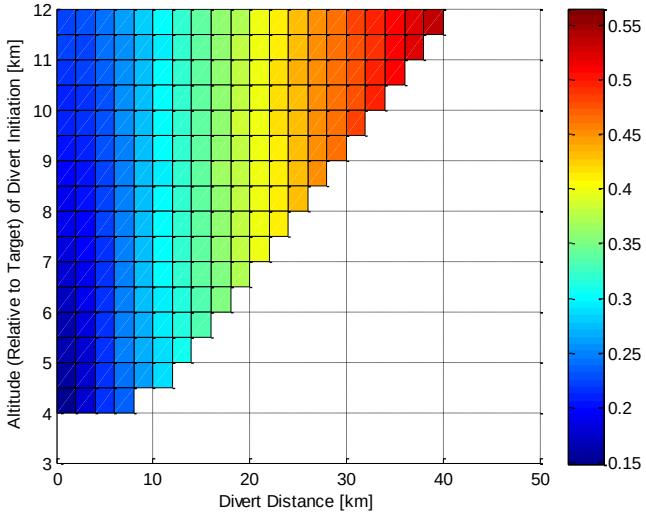

Figure 4: Propellant Mass Fraction for Various Diverts

VI. Entry Design

The entry covariance obtained from JPL corresponds to the MSL mission with TCM 5 performed. The nominal relative entry flight path angle is -15.7° for this covariance. Since MSL is a lifting entry, such a steep entry flight path angle results in a relatively high parachute deploy altitude. The ballistic entry of Smart Divert will not result in such high parachute deploy altitudes for steep entries. In order to increase altitude for ballistic entries of a given system, the entry flight path angle must be shallowed. Figure 5 shows the impact of the nominal entry flight path angle on parachute deploy MOLA altitude and landing ellipse length where each box represents a 1° change in EFPA from the nominal MSL value of -15.7°. As expected, the parachute deploy altitude decreases as the entry flight path angle is steepened. As the nominal entry flight path angle is changed, the error in entry flight path angle remains unchanged and is the same as the entry flight path angle error obtained from the original MSL covariance. Hence, the influence of the error in entry flight path angle on the landing ellipse length increases as the entry flight path angle is shallowed. This is extremely important for mission design. A shallower entry flight path angle permits high parachute deploy altitudes at the cost of an increase in landing ellipse length. Thus, in order to perform Smart Divert at high elevations, the corresponding landing ellipse length will be quite large. For the shallowest entry near -11°, the corresponding landing ellipse length is approximately 80 km, consistent with MER. Consequently, a great number of safe zones will have to be identified for high altitude parachute deploy conditions to ensure the required PMF remains reasonable. In order to provide a 5 km spread between terminal descent initiation and the ground, it is unlikely that landing site elevations greater than 2 km MOLA will be chosen for Smart Divert unless a large number of safe zones can be identified.

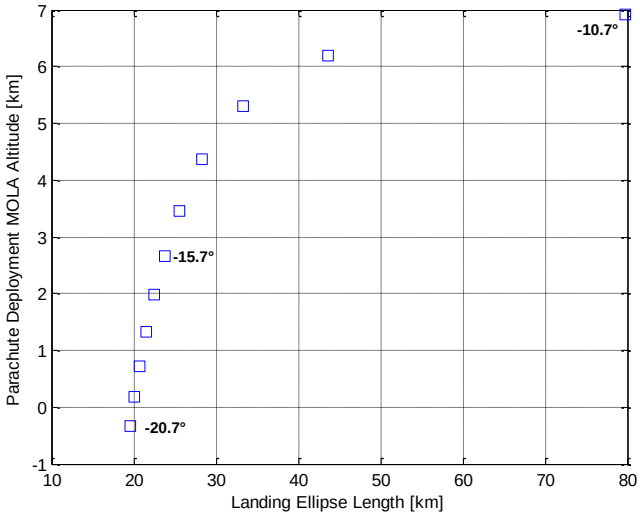

Figure 5: Parachute Deployment MOLA Altitude vs. Landing Ellipse Length for Various EFPA

VII. Performance of Smart Divert for Random Terrain

For future missions that have not been defined, the exact layout of the terrain is unknown. Consequently, the quantity and arrangement of the target landing sites are additional unknowns. A Monte Carlo was performed that included the target landing site locations as uncertain parameters. The target locations were chosen randomly from the target ellipse inside the unguided parachute deployment footprint as shown in Figure 6. A 10,000 case Monte Carlo (to obtain smooth tails of the distributions) was performed for various numbers of targets, and the resulting PMF distributions may be seen in Figure 7. As expected, the required PMF necessary to divert decreases as the number of random target locations increases. Additionally, four random sites result in a required PMF less than 0.3 for 97% of the cases assuming MSL state-of-the-art interplanetary navigation. It is important to note that a tail of the distribution does not exist on the low PMF values.

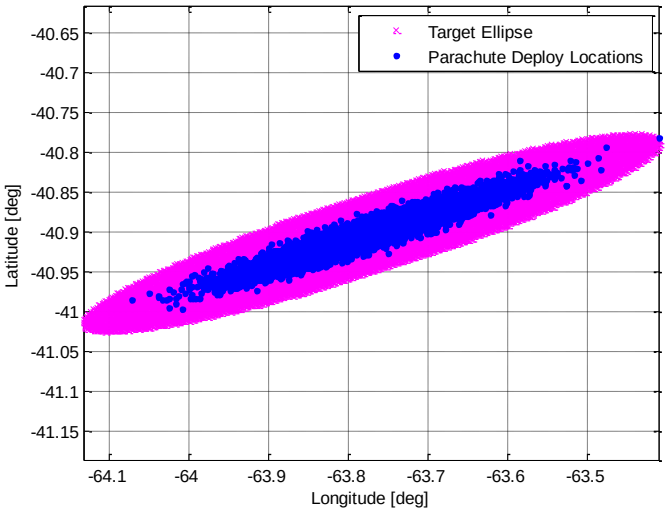

Figure 6: Target Ellipse Fitted to Parachute Deploy Locations

This is due to the choice of selecting the random sites inside the unguided parachute deployment footprint. The lower bound on PMF for each case corresponds to the PMF required for the trajectory at the toe of parachute deployment footprint to divert to the toe of the random site ellipse. In order to reduce the PMF for trajectories near the toe, sites should be selected farther downrange. This could be performed by shifting the target ellipse downrange by a specified bias.

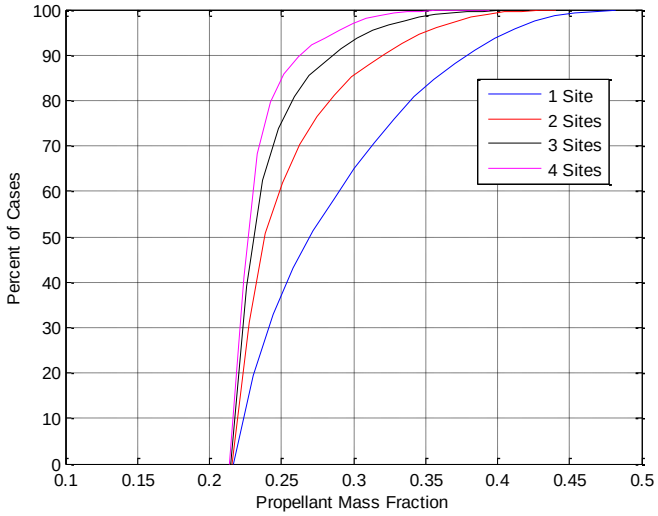

Figure 7: Cumulative Distribution Function of Propellant Mass Fraction for Various Numbers of Sites

VIII. Optimal Landing Site Arrangement

In reality, the safe zones will not be randomly placed inside the landing ellipse. Instead, mission designers will have the opportunity to arrange the safe zones in order to minimize required propellant. In order to reduce execution time, only 100 dispersed cases were used in the Monte Carlo. Similar to the random terrain analysis, the potential safe zones were chosen underneath the parachute deployment footprint resulting from the 100 case Monte Carlo. The safe zones were discretized inside target ellipse that was fitting around parachute deploy locations, see Figure 8. The optimal arrangement for various numbers of the safe zones was obtained to minimize the maximum required PMF. The optimization was performed using a grid search. This was performed to reduce computational expense when analyzing the optimal arrangement of various numbers of sites. For example, when identifying the location of one optimally placed safe zone, many iterations would have to be performed. Each iteration would require a Monte Carlo of 100 dispersed cases to be executed. This process would have to be repeated when optimizing the arrangement of two, three, or more safe zones and would result in redundant generated data as each optimization evaluates the same region of sites.

Instead of optimizing each individual case, a grid of 485 equally spaced safe zones was assessed. The Monte Carlo of 100 dispersed cases was run for each safe zone. The 48,500 entry simulations were performed in less than

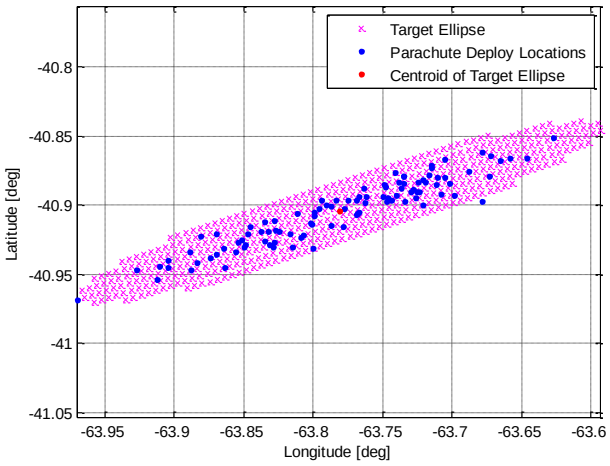

Figure 8: Potential Smart Divert Sites Fitted Around Parachute Deploy Locations

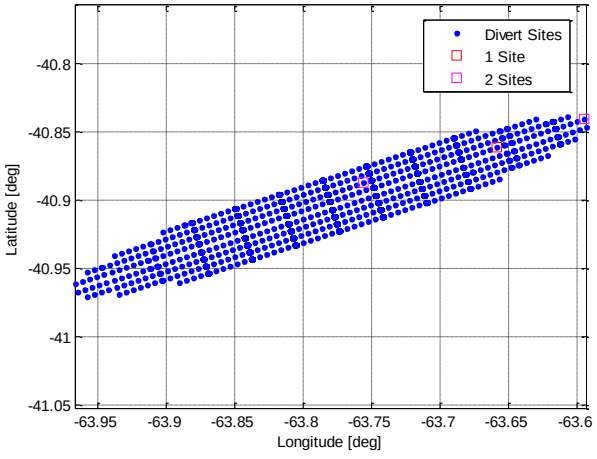

Figure 9: Divert Site Optimization

10 hours on a single computer, capitalizing on the C autocoding in Matlab and provided the data necessary to optimally arrange any number of safe zones quickly. The optimal site arrangement for various numbers of safe zones may be seen in Figure 9. As expected, the optimal arrangement consisted of divert sites located along the centerline of the target ellipse. The resulting maximum required PMF for the various number of sites may be seen in Table 3. As can be seen, two optimally arrange safe zones result in one of the safe zones placed at the toe of the ballistic parachute deployment footprint. This is due to the construction of the available safe zones directly underneath the ballistic parachute deployment footprint. Hence, the trajectory at the toe of the footprint is limiting the ability to further reduce the maximum required PMF below 0.2074, similar to that shown for the random terrain.

Table 3: Maximum Required PMF for Various Number of Safe Zones

Number of Safe Zones	Maximum Required PMF
1	0.2545
2	0.2074
3 or more	0.2074

It is clear that further analysis must be performed to understand the optimal amount of downrange bias that must be included in the placement of the target ellipse to minimize PMF. The small required PMF is also due to the rather small footprint of only approximately 20 km in major axis length originating from the 100 dispersed cases chosen for this analysis. Further analysis should include a preselected 100 cases that are chosen throughout the full 10,000 case Monte Carlo parachute deploy ellipse to properly stress the propellant required to divert to each candidate divert site during the grid search.

IX. Phoenix Example

In order to demonstrate the capability of Smart Divert for a real mission scenario, rock count data for the Phoenix landing region was obtained. A contour of the rock count data may be seen in Figure 10.[7] The red regions correspond to approximately 250 observed rocks per hectare and the dark blue regions correspond to very few observed rocks per hectare. The rock count data is constructed from observation from orbit using the High Resolution Imaging Science Experiment (HiRISE) located on the Mars Reconnaissance Orbiter (MRO). The resolution of HiRISE allows the identification of rocks 1.5 m in diameter or larger. These rocks are counted by hand and by using a computerized auto-rock counter. The rock counting is performed by identifying shadows cast by rocks and large changes in albedo caused by dust surrounding rocks. As can be seen in Figure 10, various options exist to orient the landing ellipse for Phoenix (denoted by the white and gold ellipses). It is clear that mission designers are forced to place the ellipses over regions with fewer rocks to maximize the probability of landing safely. However, not all regions of the various landing ellipse are safe with certain portions of the ellipses crossing regions with high rock counts. This is likely unavoidable due to the large landing ellipse major axis lengths of approximately 200 km caused by poor interplanetary navigation accuracy to reduce cost. Phoenix does not spin during the interplanetary transfer and uses a reaction control system (RCS) to maintain attitude, eliminating the need for a cruise stage. DDOR is used for Phoenix. However, the interplanetary geometry is not as good as the MER

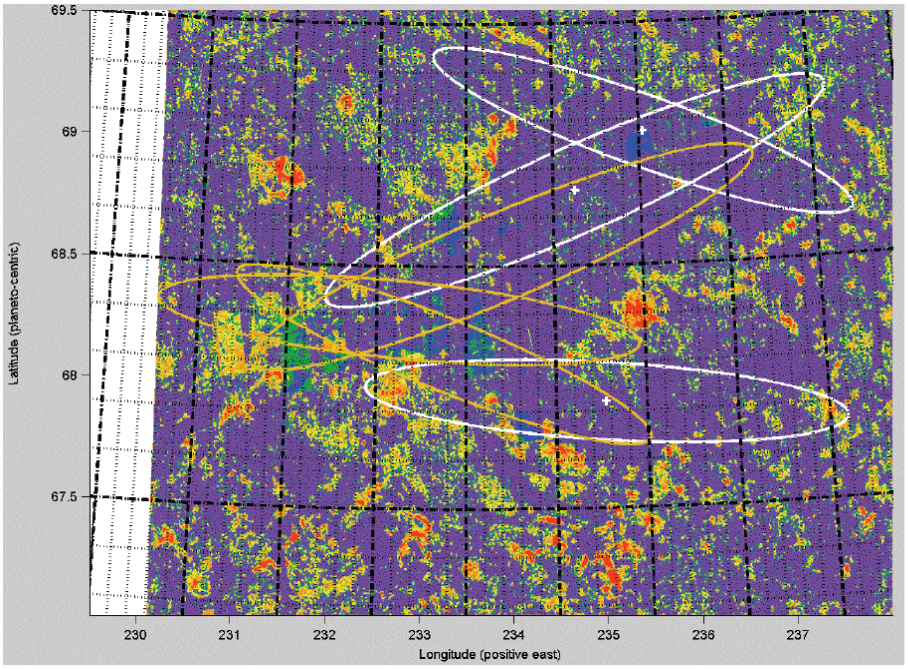

Figure 10: Phoenix Landing Region Rock Count

missions for DDOR. Hence, these measurements, although still useful, do not provide as high of navigational accuracy. This, in conjunction with cost saving measures, results in a rather large uncertainty in Phoenix delivery accuracy to Mars.

If the vehicle was capable of autonomously diverting to one of several apriori identified fuel-optimal safe zones, then landing ellipses could be placed over regions with many more rocks. Thus, Smart Divert may provide a way to land in these previously unreachable dangerous regions. A subset of the Phoenix region is shown in Figure 11. Note that the scaling of colors has changed with the red regions now corresponding to 50 rocks 1.5 m in diameter or larger per hectare. This would still be considered an extremely dangerous region to land. No previous lander, Phoenix, or MSL would be capable of safely landing in this region. However, this region might be very scientifically interesting due to rock abundance. Blue safe zone regions, denoted by magenta stars, with few rocks can be found embedded with the dangerous red regions with many rocks. The geometry of the magenta safe zones at the Phoenix landing region altitude of -4 km MOLA were preserved and placed under the ballistic parachute deploy footprint resulting from the MSL covariance, see Figure 12. At Mach 0.8, the parachute is released and the vehicle propulsively diverts to the fuel-optimal safe zone. The resulting cumulative distribution function of PMF may be seen in Figure 13. For this mission, Smart Divert requires a PMF less than 0.2 for all cases. Hence, Smart Divert is a simple EDL architecture capable of safely landing a vehicle in hazardous, scientifically interesting terrain. It is important to note that favorable PMF values were obtained by biasing the safe zones downrange from the parachute deploy ellipse as expected based on the random terrain analysis and landing site arrangement optimization.

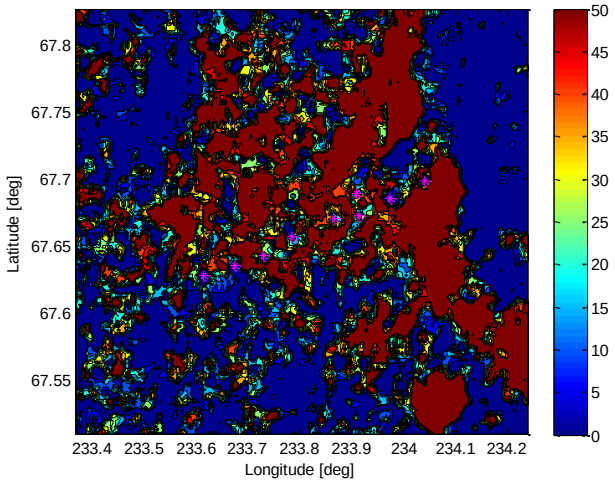

Figure 11: Subset of Phoenix Landing Site Rock Count Data per Hectare

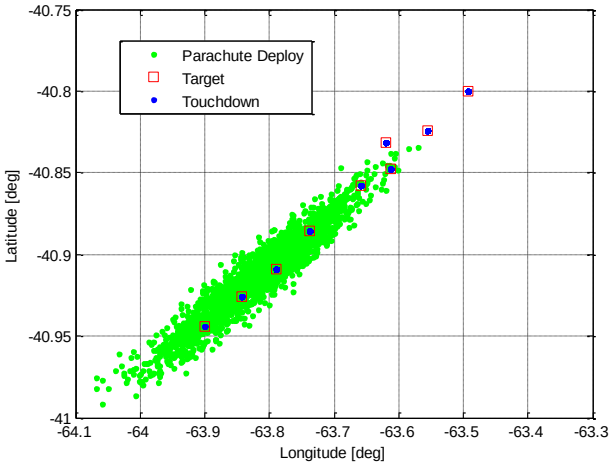

Figure 12: Snapshots of Various States

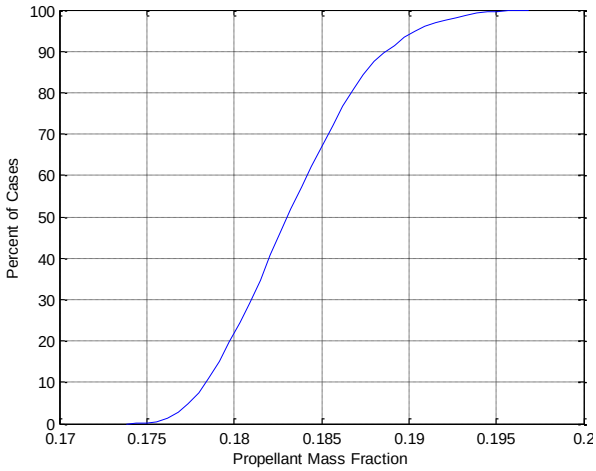

Figure 13: Cumulative Distribution Function of Propellant Mass Fraction

X. Simulator Validation

A Pathfinder test case was used to validate the developed simulation. For Pathfinder, the 585 kg vehicle entered ballistically and deployed a 12.5 m diameter supersonic disk-gap-band (DGB) parachute at a dynamic pressure of 585 Pa. At a time of 20 seconds after parachute deployment, the 64.4 kg heatshield was released. The trajectory was then propagated to the MOLA altitude immediately prior to retrorocket ignition, where the simulation was terminated. The Pathfinder entry was simulated using both the Program to Optimize Simulated Trajectories (POST) and the simulation that has been developed for this study. Figure 14 depicts both the full entry trajectory and the final phases of flight. Additionally, Table 4 compares specific trajectory event data between the two simulations. As can be seen, excellent agreement exists between both simulations.

Table 4: - Comparison of trajectory event data for Pathfinder entry

Event	POST	Simulation	% Difference
Entry			
Time (s)	0	0	0.00
Altitude (m)	128000	128000	0.00
Relative Velocity (m/s)	7479	7479	0.00
Relative Flight Path Angle (º)	-13.65	-13.65	0.00
Parachute Deploy			
Time (s)	154.5	154.3	-0.13
Altitude (m)	9916	9923	0.07
Relative Velocity (m/s)	414.5	415.2	0.17
Relative Flight Path Angle (º)	-23.35	-23.31	-0.17
Dynamic Pressure (Pa)	585.0	586.2	0.21
Heatshield Jettison			
Time (s)	174.5	174.3	-0.11
Altitude (m)	8219	8237	0.22
Relative Velocity (m/s)	90.23	90.16	-0.08
Relative Flight Path Angle (º)	-47.33	-46.56	-1.63
Dynamic Pressure (Pa)	31.98	31.88	-0.31
Trajectory Termination			
Time (s)	359.8	360.2	0.11
Altitude (m)	-2408	-2403	-0.21
Relative Velocity (m/s)	42.64	42.66	0.05
Relative Flight Path Angle (º)	-89.88	-88.83	-1.17
Dynamic Pressure (Pa)	21.55	21.55	0.00

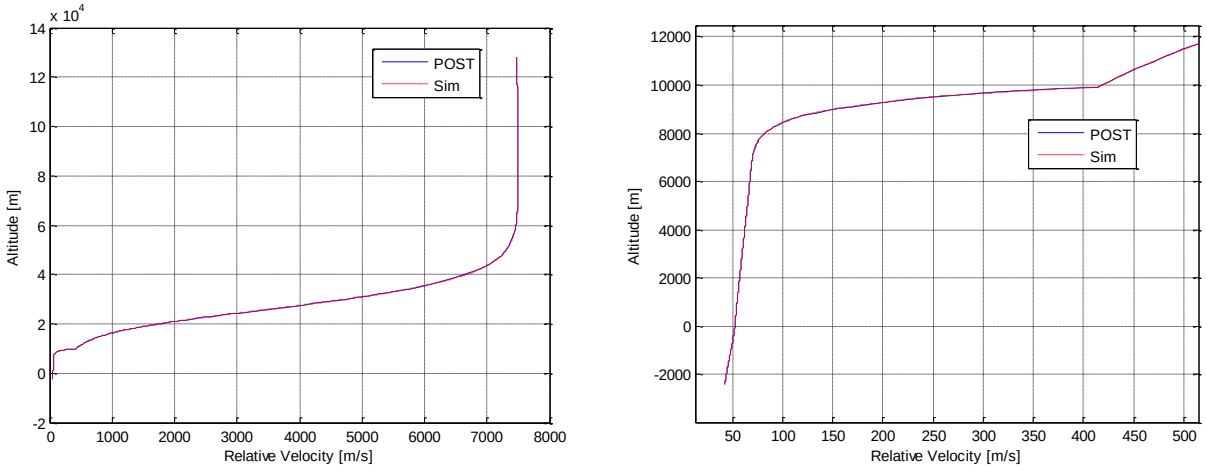

a) **b)**

Figure 14: Comparison of Developed Simulation and POST for Pathfinder Entry

XI. Conclusion

Smart Divert may enable a new, low cost EDL architecture consisting of a ballistic entry, supersonic parachute deployment, and an autonomous landing site selection. Smart Divert may also provide a simple approach to provide safe landing of vehicles in hazardous terrain. An MSL-class vehicle was studied in order to demonstrate the capability of Smart Divert for future large Mars landers. In order to restrict the required PMF to less than 0.3 a maximum divert of 10 km or less should be initiated at 5 km AGL to provide sufficient timeline for the remaining

EDL events. The altitude of the landing region governs the design of the nominal ballistic entry flight path angle. Shallower entries provide higher supersonic parachute deployment altitudes, allowing diverts to high elevations. However, shallow entries result in large landing ellipse lengths, requiring more Smart Divert safe zones to maintain reasonable PMF requirements.

The influence of number of Smart Divert sites was quantified for a random terrain in which the Smart Divert sites were randomly varied in the Monte Carlo. Four sites randomly arranged resulted in 97% of the cases requiring a PMF less than 0.3, a limit approximately double that of a gravity turn. An example method of optimal landing site arrangement showed the downrange bias necessary to optimize the maximum required PMF for one and two sites. As expected, the sites were located on the major axis of the safe zone ellipse. A downrange shift in the safe zone grid will allow optimization for more than two sites.

An example EDL scenario using rock count data from the Phoenix landing region demonstrated that Smart Divert can provide the capability to safely land entry vehicles in hazardous terrain with only a small fraction of the terrain regarded as safe. For the shown example, a minimal PMF (less than 0.2) is required to successfully perform the necessary diverts to ensure the vehicle lands safely in the hazardous terrain. Even with the introduction of hypersonic guidance for MSL, a high probability of a safe landing for this Phoenix example site could not be achieved. Hence, Smart Divert could provide the means to send vehicles to hazardous, rock populated landing areas using a simple ballistic entry followed by supersonic parachute deployment and a small divert that only minimally increases the amount of terminal descent propellant required for EDL.

XII. Future Work

It is clear that safe zones must be biased significantly downrange from the parachute deploy point to minimize the required PMF. The Smart Divert performance assessment should be expanded to incorporate flight path angle at parachute deploy to gain an understanding of what downrange bias should be used. This downrange bias should be incorporated into the random terrain analysis and landing site arrangement optimization to eliminate the trajectory at the toe of the footprint as the limiting case. This would also result in improved PMF for the random terrain analysis in which the lower PMF tail would be identified.

The influence of interplanetary navigation must also be assessed. This study assumed state-of-the-art navigation quantified in the MSL entry covariance. It is important to understand the capability of Smart Divert for cost saving, poor interplanetary navigation like that of Phoenix, resulting in large landing ellipses. Additionally, for such large landing ellipses in relatively safe terrain like that of Phoenix, the concept of Smart Divert may provide additional landing safety. Such large landing ellipse regions may contain few hazards, such as craters or large rock densities. Smart Divert may be a useful method to divert away from these dangerous exclusion zones that may sparsely exist in the large landing ellipse.

Finally, an assessment of methods to identify the fuel-optimal divert site should be performed. This analysis required an onboard evaluation of all sites by propagating simple equations of motion using the D'Souza guidance to identify the fuel-optimal safe zone. Due to the simplicity of ballistic entries, measurable entry characteristics such as peak deceleration load could potentially be used to infer the location of the vehicle inside the landing ellipse and thus can be used to select the fuel-optimal divert site without requiring the onboard propagation of equations of motion. These pre-selected sites along with measurable entry characteristics would be evaluated on the ground, eliminating the need for intelligent autonomous site selection.

References

[1] Braun, R.D. and Manning, R.M., "Mars Exploration Entry, Descent, and Landing Challenges," *Journal of Spacecraft and Rockets*, Vol. 44, No. 2, pp. 310-323, 2007.

[2] Mendeck, G.F. and Carman, G.L., "Guidance Design for Mars Smart Landers Using The Entry Terminal Point Controller," AIAA-2002-4502, AIAA Atmospheric Flight Mechanics Conference and Exhibit, 5-8 August 2002, Monterey, California

[3] Striepe, S., Way D., Dwyer, A., "Mars Science Laboratory Simulations for Entry, Descent, and Landing," Journal of Spacecraft and Rockets, Vol. 43, No.2, 2006, pp. 311-323.

[4] Steinfeldt, B.A., Grant, M.J., Matz, D.M., and Braun, R.D., "Guidance, Navigation, and Control Technology System Trades for Mars Pinpoint Landing," AIAA Atmospheric Flight Mechanics Conference, 18-21 August 2008, Honolulu, Hawaii (to be published)

[5] D'Souza, C., "An Optimal Guidance Law for Planetary Landing." Paper No. AIAA 97-3709, 1997.

[6] Wolf, A., Tooley, J., Ploen, S., Gromov, K., Ivanov, M., and Acikmese, B., "Performance Trades for Mars Pinpoint Landing," *2006 IEEE Aerospace Conference*, Paper 1661, Big Sky, Montana, March 2006.

[7] Spencer, D., "Landing Site Downselection," JPL Phoenix Mission Presentation.